Journal of Virology

A Viral Histone H4 Joins to Eukaryotic Nucleosomes and Alters Host Gene Expression

Rahul Hepat, Ji-Joon Song, Daeweon Lee and Yonggyun Kim

***J. Virol.* 2013, 87(20):11223. DOI: 10.1128/JVI.01759-13.**
Published Ahead of Print 7 August 2013.

JVI Journals.ASM.org

A Viral Histone H4 Joins to Eukaryotic Nucleosomes and Alters Host Gene Expression

Rahul Hepat,[a] Ji-Joon Song,[b] Daeweon Lee,[c] Yonggyun Kim[a]

Department of Bioresource Sciences, Andong National University, Andong, South Korea[a]; Department of Biological Sciences, KAIST, Daejeon, South Korea[b]; Department of Biology, Kyungsung University, Busan, South Korea[c]

A viral histone H4 (CpBV-H4) is encoded in a polydnavirus, *Cotesia plutellae* bracovirus. Its predicted amino acid sequence is highly homologous to that of host insect histone H4 except for an extended N-terminal tail containing 38 amino acids with nine lysine residues. Its expression induces an immunosuppression of target insects by suppressing immune-associated genes, presumably through an epigenetic control. This study analyzed its molecular interaction with eukaryotic host nucleosomes and subsequent regulation of host gene expression. Purified recombinant CpBV-H4 could associate with nucleosomal components (H2A, H2B, H3, and H4) and form an octamer. Transient expression of CpBV-H4 in an insect, *Tribolium castaneum*, was performed by microinjection of a recombinant expression vector and confirmed by both reverse transcriptase PCR (RT-PCR) and immunoblotting assays. Under this transient expression condition, total RNAs were extracted and read by a deep-sequencing technique. Annotated transcripts were classified into different gene ontology (GO) categories and compared with those of control insects injected with a truncated CpBV-H4. Target genes manipulated by CpBV-H4 expression showing significant differences (fold changes $> 10^9$) included all GO categories, including development and immune-associated genes. When the target genes were physically mapped, they were found to be scattered on entire chromosomes of *T. castaneum*. In addition, chromatin immunoprecipitation against CpBV-H4 determined 16 nucleosome sites ($P < 10^{-5}$) of the viral histone incorporation, which were noncoding regions near DNA-binding and inducible genes. These findings suggest that the viral histone H4 alters host gene expression by a direct molecular interaction with insect nucleosomes.

Nucleosomes are unit structures for eukaryotic DNA condensation. A nucleosome consists of five different histones and about 200 bp of DNA, in which the core nucleosome is formed with octamer histones of two each of H2A, H2B, H3, and H4 (1). Nucleosomes also play crucial roles in controlling gene expression by chromatin remodeling (2, 3).

A viral histone H4 (CpBV-H4) has been identified from a polydnavirus (PDV) called *Cotesia plutellae* bracovirus (CpBV) (4–6). PDVs are symbiotic to some hymenopteran insect species and help a successful parasitization by host wasps of their target lepidopteran insect hosts (7). The PDV genome is fragmented and located on their specific wasp chromosomes in a proviral form (8). Vertical transmission of PDVs, therefore, follows host wasp generations with a typical Mendelian segregation pattern (9, 10). During PDV replication, which occurs at the wasp female reproductive organ at the pupal stage, PDV genome segments become an episomal viral form (11, 12). The viral particles then move to target lepidopteran hemocoel along with the wasp egg during parasitization (13, 14). Two genera of ichnovirus (IV) and bracovirus (BV) are classified in PDVs and are different in their viral structure and host wasp families (7). Furthermore, based on the full episomal genome sequences from 6 IVs and 5 BVs, different genome compositions between IVs and BVs suggest their independent origins (15). However, both IVs and BVs alter common physiological processes of parasitized hosts, such as immunosuppression and antimetamorphosis (16).

An endoparasitoid wasp, *Cotesia plutellae*, parasitizes young larvae of the diamondback moth, *Plutella xylostella*, and alters the host immune and developmental program with the help of parasitic factors, such as teratocytes, ovarian proteins, venom proteins, and CpBV (6). A full genome sequence of an episomal form of CpBV suggests 157 candidate genes, including CpBV-H4 (17).

CpBV-H4 exhibits high sequence homologies (82.5%) with host histone H4 of *P. xylostella*, and its homologs are found in other *Cotesia*-associated BVs, such as *C. congregata* BV and *C. glomerata* BV (18). A distinct character of CpBV-H4 compared to host H4 is an extended N-terminal tail, which is a length of 38 amino acids and contains nine lysine residues (19). CpBV-H4 is located mostly in the nucleus and inhibits host immune response by suppressing expression of immune-associated genes of *P. xylostella* (19). However, a truncated CpBV-H4 deleting the extended N-terminal tail significantly loses the inhibitory activity, suggesting an epigenetic control of CpBV-H4 on host gene expression (20). Transcriptional control activity of CpBV-H4 appears to be beyond the natural target insect. Transient expression of CpBV-H4 in the beet armyworm, *Spodoptera exigua*, or in the red flour beetle, *Tribolium castaneum*, suppresses inducible expression of most antimicrobial peptide genes and significantly impairs immune responses against bacterial challenge (20, 21). Here, we have investigated an epigenetic control of CpBV-H4 against host gene expression. (i) Does CpBV-H4 directly join to eukaryotic nucleosomes? (ii) Does CpBV-H4 have specificity in the chromatin region to control specific target genes? To determine the target gene spectrum of CpBV-H4, we needed to analyze total gene expression in response to a specific expression of CpBV-H4 by a transient expression technique. A model insect for this whole-

Received 27 June 2013 Accepted 1 August 2013
Published ahead of print 7 August 2013
Address correspondence to Yonggyun Kim, hosanna@andong.ac.kr.

doi:10.1128/JVI.01759-13

genome scale study used *T. castaneum* because its total genome is sequenced and annotated (22). Before transcriptome analysis, this study showed that CpBV-H4 could be a component in nucleosomes by an *in vitro* reconstitution experiment, supporting its involvement in epigenetic control of gene expression. Then, CpBV-H4 was transiently expressed in *T. castaneum* larvae and its total transcripts were read by a short-read deep-sequencing technique (RNA-Seq). Subsequent transcriptome analysis of control and treatment determined the target genes controlled by expression of CpBV-H4. Furthermore, chromatin immunoprecipitation coupled with deep sequencing (ChIP-Seq) determined the incorporating sites of CpBV-H4 in target insect chromosomes.

MATERIALS AND METHODS

Insect culture. *T. castaneum* was reared under dry and dark conditions (a relative humidity of 60% ± 5%) at room temperature (25 ± 1°C) with wheat flour (Seoul Mill, Seoul, South Korea). Fully grown late-instar larvae (≥5 mm) were used in this study.

Preparation of recombinant CpBV-H4 (rCpBV-H4) protein. A gene encoding CpBV-H4 was cloned into a modified pET28a vector to generate N-terminal six-His-tagged CpBV-H4. pET28a-CpBV-H4 was transformed into *Escherichia coli* BL21(DE3)pLYsS cells, and the protein was expressed by adding 1 mM isopropyl β-D-1-thiogalactopyranoside at an optical density (OD) of 0.4 for 2 h. The cells expressing CpBV-H4 were harvested and were lysed with lysozyme (Sigma-Aldrich Korea, Seoul, South Korea) by incubation at 37°C for 30 min. The pellet containing CpBV-H4 was collected by centrifugation at 12,000 rpm for 40 min. The pellet was resuspended with a washing buffer containing 50 mM Tris-HCl (pH 7.5), 100 mM NaCl, 1 mM β-mercaptoethanol, and 1% Triton X-100, and the pellet was collected by centrifugation at 12,000 × *g* for 20 min. The pellet was washed with the washing buffer without 1% Triton X-100. These steps were repeated twice. Insoluble CpBV-H4 in the pellet was unfolded with an unfolding buffer containing 6 M guanidine-HCl, 20 mM sodium acetate (pH 5.2), and 5 mM dithiothreitol (DTT), incubated for 30 min while being stirred, and clarified by centrifugation at 16,000 × *g* for 10 min. The solubilized CpBV-H4 was loaded on a Sephacryl 200 XK 50/100 (2-liter) column (Sigma-Aldrich Korea) equilibrated with buffer A containing 7 M urea, 20 mM sodium acetate (pH 5.2), 5 mM β-mercaptoethanol, and 1 mM EDTA. The fractions containing CpBV-H4 were collected and loaded on TSK-SP-5PW (300-ml) ion-exchange column (Tosoh Bioscience, King of Prussia, PA) equilibrated with buffer A containing 200 mM NaCl and eluted with buffer A containing 1 M NaCl with a linear gradient. The fractions containing CpBV-H4 were collected and dialyzed against a solution containing 2 mM β-mercaptoethanol. CpBV-H4 was finally lyophilized and stored at −80°C. H2A, H2B, H3, and H4 of *Xenopus laevis* were purified as described earlier (23).

Reconstruction assay of rCpBV-H4 with nucleosome components. Two milligrams each of *X. laevis* H2A, H2B, H3, H4, and CpBV-H4 was unfolded with 1 ml of an unfolding buffer containing 6 M guanidine-HCl, 20 mM Tris-HCl (pH 7.5), and 5 mM DTT. The unfolded histone mixture was dialyzed against a refolding buffer containing 2 M NaCl, 10 mM Tris-HCl (pH 7.5), 1 mM EDTA, and 5 mM β-mercaptoethanol and loaded on a Superdex S200 column (GE Healthcare, Piscataway, NJ) equilibrated with the refolding buffer. The fractions are analyzed by 15% SDS-PAGE.

Transient expression of CpBV-H4 in larvae of *T. castaneum*. A full open reading frame (ORF) for CpBV-H4 and an open reading frame for the truncated CpBV-H4 (without the N-terminal 38 amino acids) were cloned into pIB eukaryotic expression vector (Invitrogen, Carlsbad, CA) according to previous studies (19, 21). The recombinant pIB vector was mixed with Metafectene PRO transfection reagent (Biontex, Planegg, Germany) according to the manufacturer's instructions. Briefly, 0.5-μg volumes of recombinants were mixed with 3 μl of Metafectene reagent and incubated for 20 min at room temperature to allow DNA-lipid complexes to be formed before injection into the hemocoel of late-instar larvae of *T. castaneum*. Glass capillary (World Precision Instruments, Sarasota, FL) injection needles were made using a micropipette puller PN30 (Narishige, Tokyo, Japan). A total of 60 nl was injected into the larval hemocoel at the rate 10 nl/s using a microsyringe pump controller (WPI) under a microscope (Olympus S730, Tokyo, Japan). After 48 h, total RNA was extracted using TRIzol reagent (Invitrogen), followed by reverse transcription using RT-Premix (Bioneer, Daejeon, South Korea) with an oligo(dT) and subsequent RNase H (1 U/μl) treatment. The synthesized cDNA was used as a template for PCR amplification. Control PCR was performed with an RNA extract template, which was used as a template to check for the absence of DNA contamination.

Immunoblotting. Proteins were extracted from the whole-body *T. castaneum* larvae injected with recombinant pIB-CpBV-H4 or truncated CpBV-H4 48 h postinjection (PI) and were separated by 15% SDS-PAGE. The separated proteins were electrotransferred onto an immunoblot polyvinylidene difluoride (PDVF) membrane (Bio-Rad, Hercules, CA) (24). Nonspecific sites were blocked with 5% skim milk for 1 h at room temperature. The membrane was washed thrice with phosphate-buffered saline (PBS, pH 7.4) and incubated for 1 h at room temperature with primary antibody raised against CpBV-H4 (18). After three washes with 50 mM PBS, the membrane was incubated with an anti-rabbit IgG secondary antibody (1/1,000 dilution) conjugated with alkaline phosphatase for 1 h at room temperature. Finally, after three washes with PBS, the membrane was reacted with nitroblue tetrazolium chloride-5-bromo-4-chloro-3-indolylphosphate (Sigma-Aldrich).

cDNA library preparation and deep-sequencing technique. Total RNA was extracted from *T. castaneum* larvae injected with a recombinant CpBV-H4 construct or a truncated CpBV-H4 48 h PI using TRIzol reagent. RNA quality and yield were assessed with a 2100 Bioanalyzer (Agilent Technologies, Santa Clara, CA). Briefly, mRNA was enriched by oligo(dT) magnetic beads using 1 μg of total RNA and fragmented into short sequences (200 to 700 nucleotides) by incubation with RNA fragmentation buffer (100 mM $ZnCl_2$ in 100 mM Tris-HCl, pH 7.0). The fragmented mRNAs were converted into double-stranded cDNAs by priming with random hexamer primer. After the end repair and ligation of adaptors, the products were cleaned up with AMPure beads (Beckman Coulter Genomics, Danvers, MA) to create the final cDNA library. The library was sequenced on the Illumina HiSeq 2000 (Illumina Inc., San Diego, CA) using paired end technology in 1/8 lane. Each paired-end library had an insert size of 200 to 700 bp. The average read length of 101 bp was generated as raw data.

Data processing and bioinformatics analysis. The clean reads were obtained from raw data by filtering out adaptor-only reads, reads containing more than 5% unknown nucleotides, and low-quality reads (reads containing more than 50% bases with a Q value of ≤20). The reads obtained were directly mapped to the *T. castaneum* genome (ftp://ftp.ncbi.nih.gov/genomes/tribolium_castaneum) using Bowtie (25) program (http://bowtie.cbcb.umd.edu). The python script was used to determine count numbers which belonged to a specific gene. The absolute read numbers in each gene were normalized between the control (truncated CpBV-H4) and treatment (CpBV-H4) with a TMM (trimmed mean of M-value) method (26) via the edgeR program (http://bioconductor.org). The normalized reads were then compared between the control and treatment by an exact test for the negative binomial distribution to calculate statistical significance of difference as a *P* value via the edgeR program.

GO analysis. The BLASTX algorithm with a cutoff E value of 10^{-6} was applied to the National Center for Biotechnology Information. Genes were tentatively identified according to the best hits against known sequences. Blast2GO (http://www.blast2go.org) was used to predict the functions of the sequences and to assign gene ontology GO terms.

Gene mining and RT-qPCR. Total RNA was extracted from *T. castaneum* as described above. The total RNA obtained was resuspended in 40 μl of nuclease-free water and the concentration was measured using a

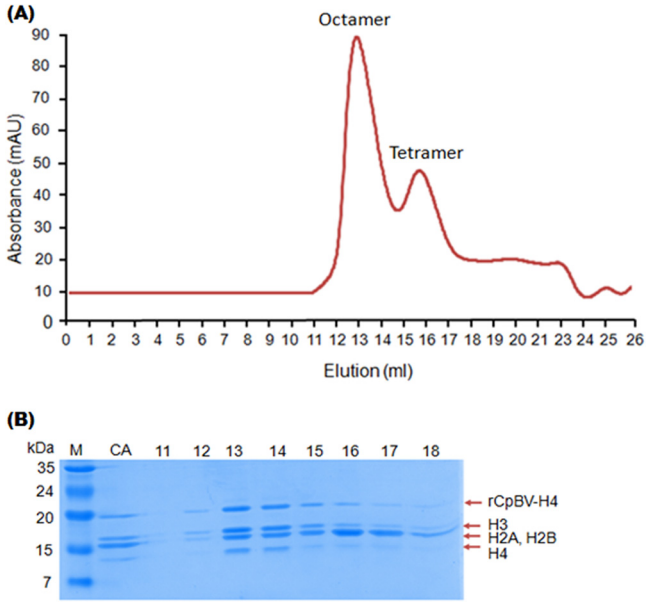

FIG 1 *In vitro* reconstruction of a viral histone H4, CpBV-H4, with eukaryotic nucleosome components. (A) Size exclusion chromatography. Two milligrams of nucleosomal components of unfolded *Xenopus laevis* H2A, H2B, H3, and H4 were mixed with unfolded CpBV-H4 in an equal concentration and refolded by dialysis against a refolding buffer (20 mM Tris [pH 7.5], 2 M NaCl, 2 mM β-mercaptoethanol, 0.5 mM EDTA) overnight. The resulting complex was then analyzed by using passage through a Supradex S20 column and monitoring absorbance at 280 nm as a function of elution volume. In the size exclusion chromatogram, two main peaks corresponded to octamer and tetramer reference. mAU, milliabsorbance units. (B) The purified fraction was analyzed by 15% SDS-PAGE. Numbers 11 to 18 represent fraction numbers of the size exclusion chromatography. M, molecular mass markers; CA, component analysis of five nucleosomal components used in the *in vitro* reconstitution assay.

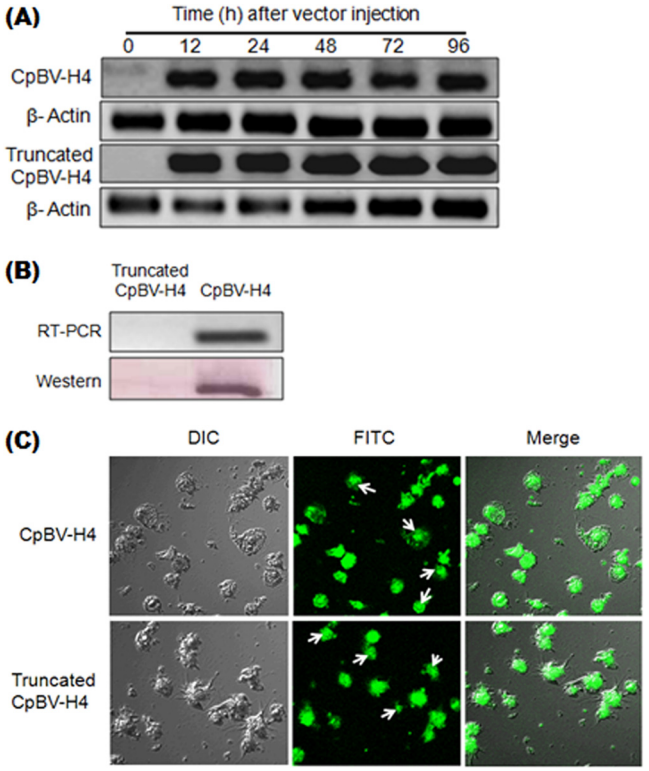

FIG 2 Transient expression of CpBV-H4 and a truncated CpBV-H4 in *Tribolium castaneum*. (A) *In vivo* transient expression of CpBV-H4 and truncated CpBV-H4. Test larvae (>5 mm) were injected with recombinant pIB construct (500 ng/larva) containing CpBV-H4 and truncated CpBV-H4. Total RNAs were collected after different intervals and analyzed by RT-PCR. β-Actin was used to confirm the integrity of the cDNA preparation. (B) Expression analysis by RT-PCR, in which primers were designed at an extended N-terminal tail. Shown is a Western blot of CpBV-H4 using a polyclonal antibody (19) raised against an extended N-terminal tail of CpBV-H4. (C) Indirect immunofluorescence assay for localization of CpBV-H4 reacted with a polyclonal antibody raised against H4 (Millipore, Billerica, MA) in hemocytes at 48 h PI using a confocal microscope (IX70; Olympus, Tokyo, Japan) at a magnification of ×400 in differential interference contrast (DIC) or fluorescein isothiocyanate (FITC) mode. Arrows indicate the viral proteins in the nucleus.

GeneQuant Pro spectrophotometer (Applied Biosystems, Carlsbad, CA). Total RNA was used as the template to synthesize first-strand cDNA as described above. The resultant cDNA was diluted to 90 ng/ml for further use in reverse transcriptase quantitative real-time PCR (RT-qPCR). Ten candidates in either of upregulated and downregulated genes were subjected to qPCR analysis with gene specific primers (data not shown). Template cDNAs were constructed as described above. The reaction mixture (20 μl) consisted of 1× Greenstar PCR master mix, 10 mM $MgCl_2$, a 0.5 mM concentration each of forward and reverse primers, and 100 ng of cDNA. The PCR condition began with activation of Hot Start *Taq* DNA polymerase by heat treatment at 95°C for 15 min and was followed by 40 cycles of 30 s at 94°C, 30 s at 55°C, and 1 min at 72°C, with a final extension for 10 min at 72°C. β-Actin was used in each sample as an internal control for equivalent of template and was amplified with forward (5′-ATGTAC CCTGGTATTGCTGAC-3′) and reverse (5′-GGACGATAGAGGGGCC AGAC-3′) primers. Fluorescence values were measured and amplification plots were generated in real time by an Exicycler program. Quantitative analysis followed a comparative threshold cycle (C_T) ($\Delta\Delta C_T$) method (27).

Physical mapping on chromosomes of *T. castaneum*. To find out the location of CpBV-H4 targets on *T. castaneum* chromosomes, the Map Viewer program (http://www.ncbi.nlm.nih.gov/mapview/) was used. Each of downregulated and upregulated genes after 10^{-3}-fold changes were then mapped individually on *T. castaneum* chromosomes by their chromosomal location.

ChIP assay. A polyclonal antibody for CpBV-H4 (18) has been used for chromatin immunoprecipitation (ChIP). Briefly, 100 larvae of *T. castaneum* injected with recombinant CpBV-H4 or truncated CpBV-H4 vectors were homogenized in PBS on ice, followed by the addition of formaldehyde (a final concentration of 1%) and incubation at 37°C for 10 min. ChIP assays were performed using a QuikChIP kit (IMGENEX, San Diego, CA) according to the manufacturer's instructions. The precipitated DNA was dissolved in Tris-EDTA buffer (10 mM Tris, 1 mM EDTA [pH 8.0]) and read by an Illumina HiSeq2000 using paired-end sequencing. Resulting reads were mapped to the *T. castaneum* genome (Tcas_3.0) (ftp://ftp.ncbi.nih.gov/genomes/tribolium_castaneum) using Bowtie (version 0.12.7) (25). Up to 2 mismatches in the seed sequence of each read were allowed, and nonunique reads were discarded by the Bowtie program. Then the overlapped reads between CpBV-H4 and truncated CpBV-H4 treatments were manually determined and deleted to determine ChIP targets. The nearest ORFs from ChIP targets were determined by the distance criterion of 1 kb.

Accession numbers. The data sets for the cDNA library from *T. castaneum* larvae injected with a recombinant CpBV-H4 construct or a truncated CpBV-H4 are available at the European Bioinformatics Institute Sequence Read Archive (EBI SRA) database with the accession number ERP001667. The ChIP reads were submitted to EBI ArrayExpress under the accession number E-MTAB-1835.

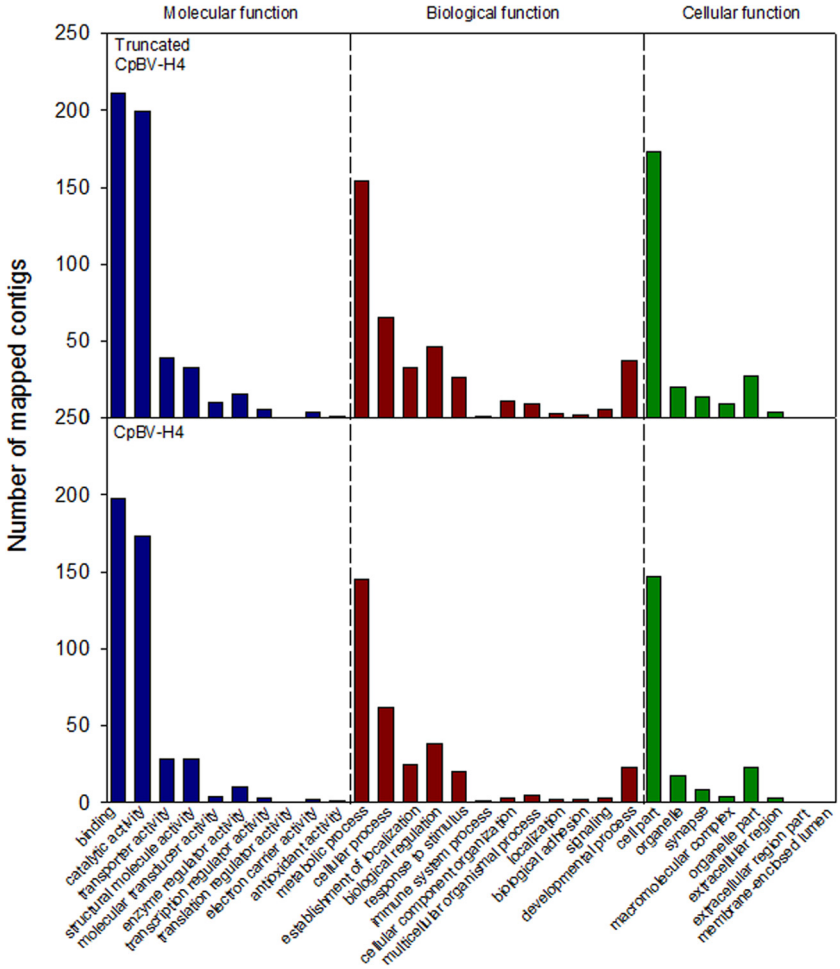

FIG 3 Effect of a viral histone H4 (CpBV-H4) on gene expression of *Tribolium castaneum* larvae by a genome-wide analysis. Test larvae (>5 mm) were microinjected with pIB expression vector (500 ng/larva) encoding CpBV-H4 (treatment) or a truncated CpBV-H4 (control). After 48 h postinjection, total RNAs were extracted and analyzed by a deep-sequencing technique. All short reads were cleaned and used for assembly to obtain contigs larger than >500 bp. The resulting 8,749 contigs of both control and treatment were used for analysis of CpBV-H4 effect on host gene expression. Total reduction of gene expression in larvae expressing CpBV-H4 was determined by comparison of total mapped contigs. Analysis of GO of control (1,386 contigs) and treatment (937 contigs) transcripts is shown. In the functional annotation, unigene sequences were first aligned using BLASTX to the NCBInr, Swiss-Prot, KEGG, and COG protein databases (E value $< 10^{-6}$), retrieving proteins with the highest sequence similarity with the given unigenes along with their protein functional annotations. We used Blast2GO program (http://www.blast2go.org) to obtain GO functional classification of unigenes.

RESULTS

A viral histone H4 joins to eukaryotic nucleosomes. A structural component of CpBV-H4 in nucleosomes was tested by analysis of its direct association with other nucleosomal components (Fig. 1). All four octamer components (H2A, H2B, H3, and H4) of *X. laevis* were mixed with purified CpBV-H4 in an equimolar concentration. Two main peaks were obtained by size exclusion chromatography (Fig. 1A). The first peak (number 13) corresponded to an octamer form and contained all four histone components and CpBV-H4 (Fig. 1B). The octamer must have consisted of two H2A, two H2B, two H3, and each of the eukaryotic H4 and the viral H4. The second peak corresponded to a tetramer form and contained mainly H2A/H2B. When CpBV-H4 was incubated with nucleosomal components lacking H4, it did not form an octamer (data not shown). These findings suggest that CpBV-H4 could interact with a histone H4 complex to be a part of a nucleosomal octamer.

Transient expression of CpBV-H4 in *T. castaneum*. We transiently expressed CpBV-H4 in *T. castaneum* (28). As a control, a truncated CpBV-H4 with a deletion of an extended 38-amino-acid-long N-terminal tail was used to address the epigenetic control of CpBV-H4 using its N-terminal extended tail (19). Both CpBV-H4 and the truncated CpBV-H4 were transiently expressed and confirmed by RT-PCR (Fig. 2A). These expressions were also observed in different tissues of hemocytes, fat body, gut, and epidermis (data not shown). A specific antibody against the extended N-terminal tail recognized only CpBV-H4 and not the truncated CpBV-H4 (Fig. 2B). The transiently expressed CpBV-H4s were localized in the nuclei of *T. castaneum* hemocytes (Fig. 2C).

Transient expression of CpBV-H4 modulates host gene expression. To test the effect of CpBV-H4 expression on host gene expression, total RNAs of *T. castaneum* larvae expressing CpBV-H4 or the truncated CpBV-H4 were read by a deep-sequencing technique (Fig. 3). After sequence quality screening, total mapped reads were 4,063,173 from the larvae expressing CpBV-H4 and 4,808,909 from the larvae expressing the truncated

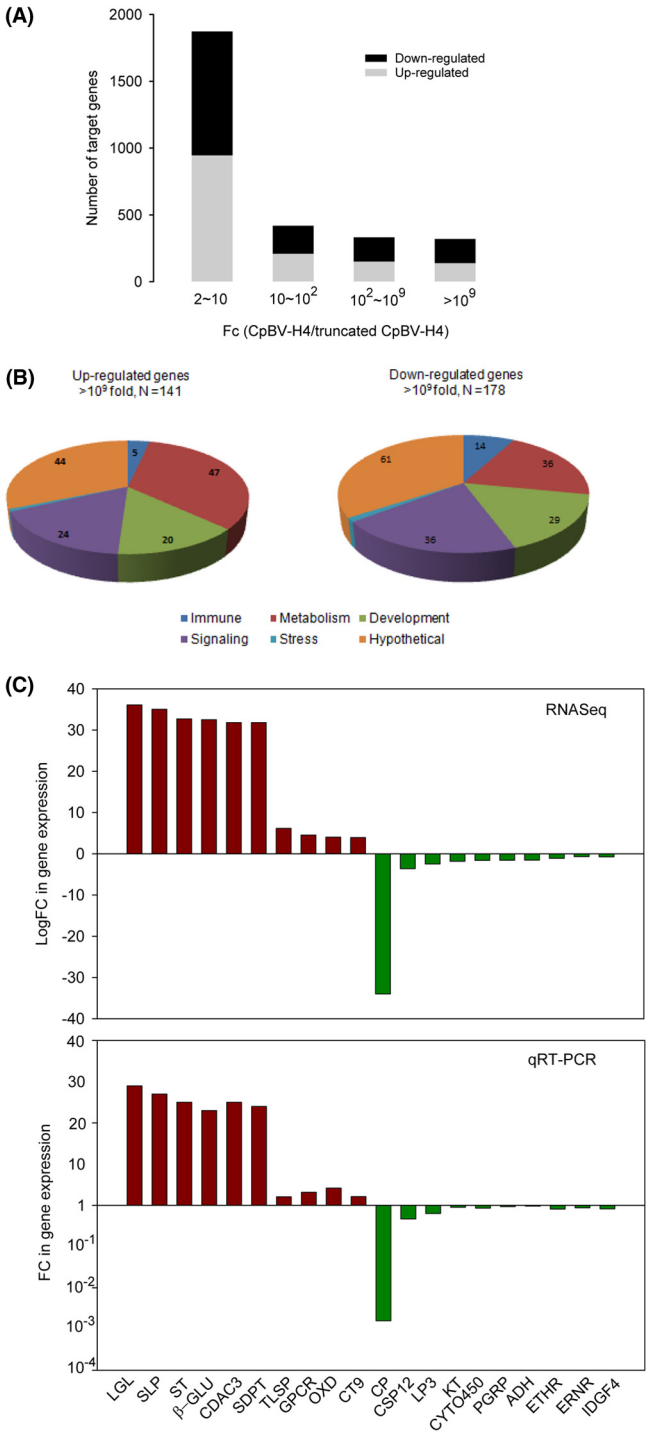

FIG 4 Analysis of host gene expression alterations of *Tribolium castaneum* larvae by a transient expression of a viral histone H4, CpBV-H4. Normalized read numbers of annotated host genes were used to compare transcript levels between control (a truncated CpBV-H4) and treatment (CpBV-H4). (A) Target host genes of CpBV-H4. Based on fold change (FC), host genes changed in expression levels by CpBV-H4 expression are grouped into weak (>2 to ~10 FC), moderate (>10 to ~10^2 FC), strong (>10^2 to ~10^9 FC), and highly strong (>10^9 FC) targets. (B) Functional grouping of highly strong target genes of *T. castaneum*. (C) RT-PCR and Illumina RNA-Seq comparison. Expression levels of 20 genes selected in their differential pattern (upregulated and downregulated) were detected by real-time PCR (RT-PCR) and compared with RNA-Seq fold change. LGL, SLP, ST, β-GLU, CDAC3, SDPT, TLSP, GPCR, OXD, CT9, CP, CSP12, LP3, KT, CYTO450, PGRP, ADH, ETHR, ERNR, and IDGF4 represent lactoylglutathione lyase, spaetzle-like protein, sulfotransferase, β-glucosidase, chitin deactylase 3, sodium-dependent potassium transporter, trypsin-like serine protease, G protein-coupled receptor, oxidase/peroxide, chitinase 9, cuticle protein, chemosensory protein 12, lipase 3, kaptin, cytochrome P450, peptidoglycan receptor protein, alcohol dehydrogenase, ecdysone-triggering hormone receptor, ecdysone nuclear receptor, and imaginal disc growth factor 4 of *T. castaneum*, respectively.

CpBV-H4. These short reads were then assembled, and subsequent contig sequences were used for gene annotation. Based on GO analysis, expression profiles of control and CpBV-H4 treatment were not significantly different in molecular function ($\chi^2 = 3.9$; $df = 9$; $P = 0.9174$), biological process ($\chi^2 = 7.1$; $df = 11$; $P = 0.7876$), or cellular process ($\chi^2 = 0.5$; $df = 7$; $P = 0.991$).

To determine target genes controlled in their expression by CpBV-H4, normalized fold changes between control (a truncated CpBV-H4) and treatment (CpBV-H4) larvae were assessed (Fig. 4). Among the assembled genes, 19% showed more than a two-fold difference in expression levels due to CpBV-H4 (Fig. 4A). These target genes included both upregulated (50.5%) and downregulated (49.5%) expression patterns in response to CpBV-H4 expression. The hottest targets (>10^9-fold changes) were compared between upregulated and downregulated genes in their annotated composition, in which both groups were not significantly different ($\chi^2 = 8.6$; $df = 5$; $P = 0.1223$) in gene numbers classified into GO subcategories (Fig. 4B). To confirm the fold changes estimated from a deep-sequencing technique, we selected 20 genes which were different in expression patterns (Fig. 4C). Expressions of these selected genes were analyzed by RT-qPCR with gene-specific primers, which clearly supported the fold change estimation of RNA-Seq method to estimate gene expression levels.

Scattered targets of CpBV-H4 in host chromosomes. Target genes (>10-fold change in expression) were physically mapped on chromosomes of *T. castaneum* (Fig. 5). Target genes were scattered on all 10 chromosomes, in which some target genes were on mitochondrial DNA (data not shown). To understand the scattered target pattern, ChIP was performed in both control (a truncated CpBV-H4) and treatment (CpBV-H4) larvae. All ChIP DNA segments were read by a deep-sequencing technique. After removal of genes overlapped with control, 16 ChIP targets of CpBV-H4 were determined with a cutoff P value of 10^{-5} and showed that they were also localized on all chromosomes of *T. castaneum*.

These 16 ChIP target sites were further analyzed in their regions of sequence homology and the neighboring genes (Table 1). When 16 ChIP target sites were aligned, they did not show any conserved sequence motif except variable AT-rich motifs (data not shown). All 16 ChIP sites were not localized in open reading frames. Among neighboring genes within ≈1 kb from the ChIP targets, seven genes are predicted to be associated with gene expression control by binding affinity to DNA, four genes with metabolism, three genes with detoxification, and two genes with immune and nerve processes. It is notable that one of the ChIP targets was histone deacetylase (HDAC), which was the most greatly modulated in its expression among 16 ChIP target genes.

DISCUSSION

A viral histone H4, CpBV-H4, is highly conserved in its amino acid sequence with its host histone H4 except for an extended 38-amino-acid N-terminal tail (18). This N-terminal tail contains

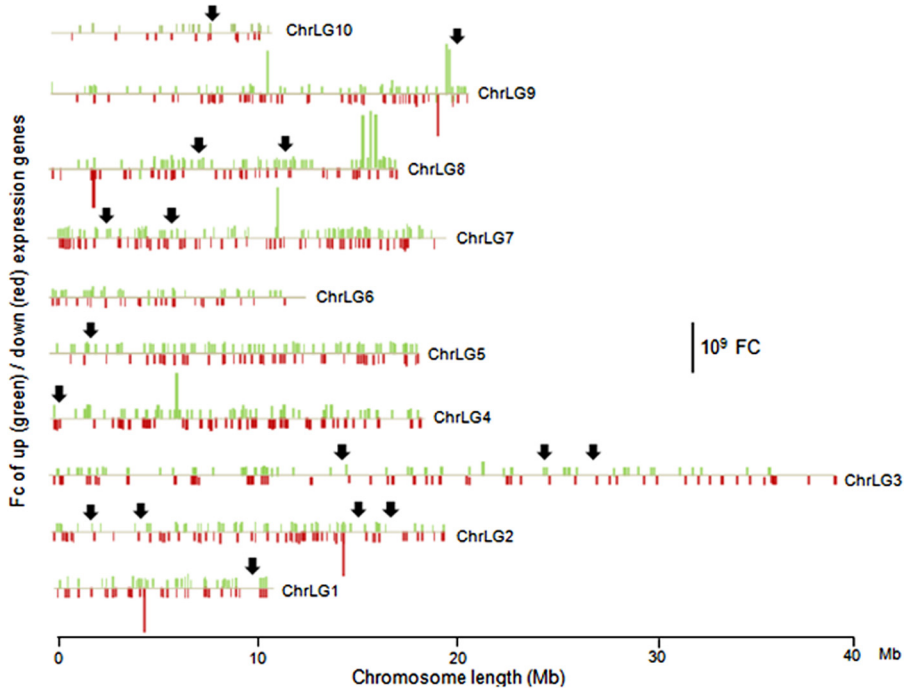

FIG 5 Physical mapping of target genes (>10-fold change [FC]) regulated by CpBV-H4 on chromosomes of *Tribolium castaneum*. Locations of CpBV-H4 incorporated into host nucleosomes were analyzed by ChIP. ChIP sites are indicated with arrows. Ten chromosomes are presented in linkage groups (ChrLGs).

nine lysine residues, suggesting extensive covalent modification to modulate nucleosome conformation if the viral histone H4 can join to form a core octamer. This study experimentally proved that the viral histone H4 joined to form an octamer with endogenous octamer components (H2A, H2B, H3, and H4) derived from *X. laevis*. The sequence homologies between *X. laevis* and *P. xylostella* are 96.8% for H2A, 78.2% for H2B, 100.0% for H3, and 99.0% for H4. The sequence homologies between *X. laevis* and *T. castaneum* are 66.2% for H2A, 12.1% for H2B, 10.0% for H3, and 89.3% for H4. Interestingly, without eukaryotic H4 in the reconstruction assay, the viral H4 alone could not form an octamer with H2A, H2B, and H3. Furthermore, eukaryotic H4 and viral H4 were apparently equimolar in octamers formed in an *in vitro* assay based on the total octamer molecular weight and the gel intensity. This suggests that H3 may discriminate viral H4 from eukaryotic H4. Thus, the viral octamer may be reconstructed only from a heterodimeric mixture of eukaryotic H4-H3 and viral H4-H3 to form a core tetramer kernel (29). Furthermore, an H2A-H2B heterodimer formed in a reconstitution experiment in the presence of the viral histone H4 suggests that the viral histone H4 may play a

TABLE 1 Binding sites of CpBV-H4 in *Tribolium castaneum* chromosomes from an analysis of chromatin immunoprecipitation followed by deep sequencing

ChIP target (location on chromosome)	Distance (bp)[a] to nearest ORF	Nearest ORF of CpBV-H4 (GenBank accession no.)	Fold change[b]	Predicted function
ChrLG9 (678288–878523)	−201	Zinc finger protein (NM_001170615)	1.5	Gene expression
ChrLG7 (641556–641805)	−249	CCAT enhancer-binding protein (XM_962431)	0.4	Gene expression
ChrLG2 (163078–163822)	+685	AT-rich interaction domain (XM_963021)	29.0	Gene expression
ChrLG7 (184553–184644)	+91	Coiled-coil-containing protein (XM_971120)	23.0	Gene expression
ChrLG3 (40711–40928)	−217	Histone deacetylase (XM_961540)	64.0	Gene expression
ChrLG3 (168175–168581)	−406	Eukaryotic translation initiation factor 6 (XM_964804)	50.0	Gene expression
ChrLG8 (184644–184853)	−211	Mitogen-activated kinase protein (XM_963454)	50.0	Gene expression
ChrLG5 (312840–313042)	−202	Imaginal disc growth factor 2 (NM_001044627)	0.8	Gene expression
ChrLG2 (444266–444473)	−462	Cytochrome P450 (XM_968526)	50.0	Detoxification
ChrLG2 (351868–352086)	−994	Glutathione *S*-transferase (JN695809)	50.0	Detoxification
ChrLG3 (253140–253343)	−1023	Alcohol dehydrogenase (XM_961796)	33.3	Detoxification
ChrLG4 (256274–256522)	−248	Ubiquinol-cytochrome C reductase (XM_965278)	45.0	Metabolism
ChrLG2 (141873–142075)	−202	Geranyltransferase (XM_964589)	12.0	Metabolism
ChrLG8 (641556–641805)	−249	*S*-Adenosylmethionine decarboxylase (XM_962180)	0.7	Metabolism
ChrLG1(384–724)	−340	Prophenoloxidase-activating factor (XM_963175)	33.3	Immune
ChrLG10 (466313–466512)	−199	Metabotropic GABA-B receptor (XM_964268)	50.0	Nerve

[a] "+" and "−" represent locations upstream and downstream from the nearest ORF.
[b] Fold change in gene expression between CpBV-H4 and control.

role in forming an octamer by interacting with H2A-H2B heterodimer just like eukaryotic histone H4 because each H2A-H2B heterodimer binds to an H4-H3 tetramer through contacts between H2B and H4 (30). However, the fact that the viral histone H4 alone did not form an octamer suggests that its extended N-terminal tail may limit a favorable interaction with H2A-H2B heterodimers when the viral histone H4 coexists at an octamer.

Transient expression of CpBV-H4 in *T. castaneum* resulted in its expression and localization mostly in the nucleus. A previous study showed that parasitized *P. xylostella* (natural host) expressed CpBV-H4, most of which was also detected in the nucleus (18, 19). Thus, *in vitro* nucleosome reconstruction and *in vivo* nucleus localization of CpBV-H4 suggested its altering effect on host gene expression. To test this hypothesis, this study used a transient expression of CpBV-H4 in *T. castaneum* larvae. To determine an epigenetic control action of CpBV-H4, this study also transiently expressed a truncated CpBV-H4 as a control by deleting its extended N-terminal tail. After confirmation of both expressions of wild and mutant CpBV-H4, a quantitative and qualitative change in transcriptome on a genome-wide scale was analyzed by RNA-Seq using a deep-sequencing technique. The total number of mapped reads was lower (84.5%) in CpBV-H4-expressing larvae than in control larvae. However, overall expression profiles in three main categories were not different between the control and treatment. This suggests a multitarget control of CpBV-H4 against host gene expression with somewhat overall suppression. In fact, the target genes, which were significantly modulated in expression levels by CpBV-H4 expression, were mapped and located on entire chromosomes of *T. castaneum*. ChIP-Seq analysis determined 16 target binding sites of CpBV-H4 to *T. castaneum* chromatins. Interestingly, neighboring genes of these binding sites included inducible or regulating genes presumably functionally associated with gene expression control, detoxification, metabolism, and immune or neural processes. One of the ChIP targets included histone deacetylase, which was upregulated by expression of CpBV-H4. The histone amino termini (15 to 38 residues in length) extend from the core and form the histone "tails," where they can be subjected to enzyme-catalyzed, post-translational modifications (31), which affect their charge and function. Usually, specific N-terminal lysines of H4 can be acetylated at ε-amino groups by a family of enzymes, the histone acetyltransferase (HAT) (32). For example, acetylation of lysine 16 of histone H4 induces higher-order chromatin structure and allows functional interactions between a nonhistone protein and the chromatin fiber (33). Histone acetylation is reversed by HDACs, which can also mediate gene interaction as components of large complexes in a variety of eukaryotes (34). Several transcriptional activators or repressors form complexes with HATs or HDACs in particular regions of chromatin and regulate gene activity (3, 35). Thus, the modulation of HDAC expression by CpBV-H4 may lead to an overall expression control against multitarget genes.

The fact that the ChIP target genes appear to be inducible in their expression in response to internal and external signal or stress suggests that CpBV-H4 may join to nucleosomes undergoing chromatin remodeling probably by reassembly of histone subunits. Earlier studies showed that CpBV-H4 is expressed during entire period of *P. xylostella* parasitization by *C. plutellae* (18). CpBV-H4 expression also suppressed the expression of host histone H4 of *P. xylostella* (19). Thus, the persistent expression of CpBV-H4 and the subsequent decrease in expression of host histone H4 suggest that the viral histone H4 may have more of a chance to join to host nucleosomes with developmental progress of parasitism within the parasitized host. This increase of viral histone H4 joining to host nucleosomes may result in a massive expression control of host genes associated with host development and immune responses. Parasitized *P. xylostella* fails to undergo a larva-to-pupa metamorphosis due to a lack of nutritional supply, which prevents the parasitized larvae from reaching the critical body size for pupal metamorphosis (36, 37). About 26% mapped target genes ($>10^9$-fold change in upregulation, 46 out of 141 genes, and in downregulation, 36 out of 178 genes) of CpBV-H4 were associated with metabolism in this study. Moreover, parasitized *P. xylostella* larvae exhibit significant immunosuppression, in which expression of cellular and humoral immune genes is inhibited by CpBV-H4 expression (18, 20). The transient expression of CpBV-H4 also inhibited expression of these immune-associated genes in *T. castaneum* larvae (21). Thus, CpBV-H4 can be a main persistent parasitic factor in *C. plutellae* parasitism by altering the expression of the inducible genes related with immune and development of the parasitized *P. xylostella*.

In summary, a viral histone H4 derived from a polydnavirus can join to nucleosomes. The joining sites of the viral histone H4 are not conserved, but they appear to be located near inducible or regulatory genes. Its control of host gene expression includes all functional categories. Its expression in parasitized *P. xylostella* may result in entire alteration of host gene expression toward favorable conditions for parasitoid development while preventing the development and immune response of the parasitized host. Similar viral histone H4s are encoded in other *Cotesia*-associated polydnaviral genomes (4, 18) but are not known in other groups of PDVs. This suggests that the origin of these viral histone H4s may be host wasp histone H4. It would be interesting to trace how the viral histone H4 has evolved to have a unique extended N-terminal tail, which is a critical molecular structure to perform its epigenetic control.

ACKNOWLEDGMENTS

This study was supported by a grant (2011-0013069) to Y.K. from National Research Foundation of Korea. A partial grant was also supported by the Next-Generation Biogreen 21 program (PJ009020) of the Rural Development Administration, Suweon, South Korea, to D.L.

REFERENCES

1. **Wolffe AP.** 1992. Chromatin: structure and function. Academic Press, San Diego, CA.
2. **Turner BM.** 1993. Decoding the nucleosome. Cell **759:**5–8.
3. **Grunstein M.** 1997. Histone acetylation in chromatin structure and transcription. Nature **389:**349–352.
4. **Espagne E, Dupuy C, Huguet E, Cattolico L, Provost B, Martins N, Poirié M, Periquet G, Drezen JM.** 2004. Genome sequence of a polydnavirus: insights into symbiotic virus evolution. Science **306:**286–289.
5. **Ibrahim AMA, Choi JY, Je YH, Kim Y.** 2005. Structure and expression profile of two putative *Cotesia plutellae* bracovirus genes (CpBV-H4 and CpBV-E94α) in parasitized *Plutella xylostella*. J. Asia Pac. Entomol. **8:**359–366.
6. **Kim Y, Choi JY, Je YH.** 2007. *Cotesia plutellae* bracovirus genome and its function in altering insect physiology. J. Asia Pac. Entomol. **10:**181–191.
7. **Webb BA, Beckage NE, Hayakawa Y, Krell PJ, Lanzrein B, Stoltz DB, Strand MR, Summers MD.** 2000. Polydnaviridae, p 253–260. *In* van Regenmortel MHV, Fauquet CM, Bishop DHL, Carstens EB, Estes MK, Lemon SM, Maniloff J, Mayo MA, McGeoch DJ, Pringle CR, Wickner RB (ed), Virus taxonomy: seventh report of the International Committee on the Taxonomy of Viruses. Academic Press, San Diego, CA.
8. **Krell PJ, Summers MD, Vinson SB.** 1982. Virus with a multipartite

superhelical DNA genome from the ichneumonid parasitoid *Campoletis sonorensis*. J. Virol. **43:**859–870.
9. **Stoltz DB.** 1990. Evidence for chromosomal transmission of polydnavirus DNA. J. Gen. Virol. **71:**1051–1056.
10. **Whitfield JB.** 2000. Phylogeny of microgastroid braconid wasps, and what it tells us about polydnavirus evolution, p 97–105. *In* Austin AD, Dowton M (ed), The Hymenoptera: evolution, biodiversity and biological control. CSIRO, Melbourne, Australia.
11. **Belle E, Beckage NE, Rousselet J, Poirié M, Lemeunier F, Drezen JM.** 2002. Visualization of polydnavirus sequences in a parasitoid wasp chromosome. J. Virol. **76:**5793–5796.
12. **Wyder S, Tschannen A, Hochuli A, Gruber A, Saladin V, Zumbach S, Lanzrein B.** 2002. Characterization of *Chelonus inanitus* polydnavirus segments: sequences and analysis, excision site and demonstration of clustering. J. Gen. Virol. **83:**247–256.
13. **Theilmann DA, Summers MD.** 1986. Molecular analysis of *Campoletis sonorensis* virus DNA in the lepidopteran host *Heliothis virescens*. J. Gen. Virol. **67:**1961–1969.
14. **Theilmann DA, Summers MD.** 1988. Identification and comparison of *Campoletis sonorensis* virus transcripts expressed from four genomic segments in the insect hosts *Campoletis sonorensis* and *Heliothis virescens*. Virology **167:**329–341.
15. **Volkoff AN, Jouan V, Urbach S, Samain S, Bergoin M, Wincker P, Demettre E, Cousserans F, Provost B, Coulibaly F, Legeai F, Beliveau C, Cusson M, Gyapay G, Drezen JM.** 2010. Analysis of virion structural components reveals vestiges of the ancestral ichnovirus genome. PLoS Pathog. **6:**e1000923.
16. **Webb B, Strand MR.** 2005. The biology and genomics of polydnaviruses, p 323–360. *In* Gilbert L, Iatrou K, Gill SS (ed), Comprehensive molecular insect science, vol 6. Elsevier, Amsterdam, Netherlands.
17. **Chen YF, Gao F, Ye XQ, Wei SJ, Shi M, Zheng HJ, Chen X.** 2011. Deep sequencing of *Cotesia vestalis* bracovirus reveals the complexity of a polydnavirus genome. Virology **414:**42–50.
18. **Gad W, Kim Y.** 2008. A viral histone H4 encoded by *Cotesia plutellae* bracovirus inhibits hemocyte-spreading behaviour of the diamondback moth, *Plutellae xylostella*. J. Gen. Virol. **89:**931–938.
19. **Gad W, Kim Y.** 2009. N-terminal tail of a viral histone H4 encoded in *Cotesia plutellae* bracovirus is essential to suppress gene expression of host histone H4. Insect Mol. Biol. **18:**111–118.
20. **Kim J, Kim Y.** 2010. Transient expression of a viral histone H4, CpBV-H4 suppresses immune-associated genes of *Plutella xylostella* and *Spodoptera exigua*. J. Asia Pac. Entomol. **13:**313–318.
21. **Hepat R, Kim Y.** 2011. Transient expression of a viral histone H4 inhibits expression of cellular and humoral immune-associated genes in *Tribolium castaneum*. Biochem. Biophys. Res. Commun. **415:**279–283.
22. **Zou Z, Evans JD, Lu Z, Zhao P, Williams M, Sumathipala N, Hetru C, Hultmark D, Jian HN.** 2007. Comparative genomic analysis of the *Tribolium* immune system. Genome Biol. **8:**R177. doi:10.1186/gb-2007-8-8-r177.
23. **Dyer PN, Edayathumangalam RS, White CL, Bao Y, Chakravarthy S, Muthurajan UM, Luger K.** 2004. Reconstitution of nucleosome core particles from recombinant histones and DNA. Methods Enzymol. **375:**23–44.
24. **Towbin H, Staehelin T, Gordon J.** 1979. Electrophoretic transfer of proteins from polyacrylamide gels to nitrocellulose sheets: procedure and some applications. Proc. Natl. Acad. Sci. U. S. A. **76:**4350–4354.
25. **Langmead B, Trapnell C, Pop M, Salzberg SL.** 2009. Ultrafast and memory-efficient alignment of short DNA sequences to the human genome. Genome Biol. **10:**R25. doi:10.1186/gb-2009-10-3-r25.
26. **Robinson MD, Oshlack A.** 2010. A scaling normalization method for differential expression analysis of RNA-seq data. Genome Biol. **11:**R25. doi:10.1186/gb-2010-11-3-r25.
27. **Livak KJ, Schmittgen TD.** 2001. Analysis of relative gene expression data using real-time quantitative PCR and the $2^{-\Delta\Delta CT}$ method. Methods **25:**402–408.
28. **Hepat R, Kim Y.** 2012. *In vivo* transient expression for the functional analysis of polydnaviral genes. J. Invertebr. Pathol. **111:**152–159.
29. **Arents G, Burlingame RW, Wang BC, Love WE, Moudrianakis EN.** 1991. The nucleosomal core histone octamer at 3.1 Å resolution: a tripartite protein assembly and a left-handed superhelix. Proc. Natl. Acad. Sci. U. S. A. **88:**10148–10152.
30. **Luger K, Mäder AW, Richmond RK, Sargent DF, Richmond TJ.** 1997. Crystal structure of the nucleosome core particle at 2.8 Å resolution. Nature **389:**251–260.
31. **Wu RS, Panusz HT, Hatcj CL, Bonner WM.** 1986. Histones and their modifications. CRC Crit. Rev. Biochem. **20:**201–263.
32. **Kuo MH, Allis CD.** 1998. Roles of histone acetyltransferases and deacetylases in gene regulation. Bioessays **20:**615–626.
33. **Shogren-Knaak M, Ishii H, Sun JM, Pazin MJ, Davie JR, Peterson CL.** 2006. Histone H4-K16 acetylation controls chromatin structure and protein interactions. Science **311:**844–847.
34. **Pazin M, Kadonaga J.** 1997. What's up and down with histone deacetylation and transcription? Cell **89:**325–328.
35. **Turner BM.** 1993. Decoding the nucleosome. Cell **75:**5–8.
36. **Kwon B, Kim Y.** 2008. Transient expression of an EP1-like gene encoded in *Cotesia plutellae* bracovirus suppresses the hemocyte population in the diamondback moth, *Plutella xylostella*. Dev. Comp. Immunol. **32:**932–942.
37. **Kim J, Kim Y.** 2010. A viral histone H4 suppresses expression of a transferrin that plays a role in the immune response of the diamondback moth, *Plutella xylostella*. Insect Mol. Biol. **19:**567–574.